Optica Applicata VIII/2, 1978

Jiři Janta*, Miroslav Miler*, Rudolf Vrabec**

Radial vibrations of piezoceramic resonators investigated by holographic interferometry***

Three lowest radial vibration modes of circular piezoceramic plates were investigated by the method of time-average holographic interferometry. The experimental conditions are discussed and the optimum arrangement chosen. A satisfactory agreement of the results with common approximate theory of radial vibrations was obtained. The thickness vibrations accompanying the radial ones were also investigated.

1. Introduction

Time-average method of holographic interferometry [1] can be advantageously used for visualization of vibrational states of mechanical resonators. In contradistinction to classical method of Chladni figures it gives information not only on knot-lines position on the surface of the vibrating objects, but also on the magnitude and direction of the vibrations in all surface points. Provided that a proper experimental arrangement is used one can determine even various components of the amplitude in particular points, and thus distinguish superimposed vibration modes.

A great deal of papers (e.g. [2, 3, 4]) were concerned with various aspects of investigation of the mechanical vibrations, being concentrated mainly on the vibrations perpendicular to the surface of the objects. In this contribution the application of the time-average method to the experimental study of radial vibrations of simple piezoceramic resonators is presented. The in-plane vibrations lead to certain complications during experiment and evaluation of the interferograms if compared with vibrations perpendicular to the surface. For the sake of simplification and illustrativeness of the evaluation the method of comparison of experimental interferograms with corresponding model interferograms will be used.

*) Institute of Radio Engineering and Electronics, Czechoslovak Academy of Sciences Prague, Czechoslovakia.

**) TESLA, Hradec Králové, Czechoslovakia.

***) The tentative version of the paper was presented at the 2nd Symposium on Applied Holography INTERKAMERA, Prague 1976.

2. Experimental interferograms

The samples used in our experiments were manufactured by TESLA Hradec Králové from Pb(Zr, Ti)O_3-ceramics PKM 10 with the following parameters: density $\varrho = 7.4\times 10^{-3}$ kg·m^{-3}, elastic modulus $Y^E_{11} = 0.94\times 10^{-11}$ N·m^{-2}, Poisson's ratio $\sigma \approx \approx 0.30$. Circular plates with diameters $2R = 50$ mm, and thicknesses $t = 2$ and 8 mm were prepared.

Both the plates were polarized perpendiculary to their faces, which were covered with electrodes. The frequency constant of the basic mode is $N_{r1} = (2.3\pm \pm 0.1)$ kHz·m [5].

Vibrations of the plates were excited with a power generator with output impedance 75 Ω. By electrical measurement three lowest resonant frequencies were found, namely $f_r = 47$, 125, and 200 kHz for the thin plate and $f_r = 46.5$, 115, and 265 kHz for the thick plate. In both cases, the first frequencies correspond to the basic radial mode according to the relation

$$f_{r1} = \frac{N_{r1}}{2R} = (46\pm 2)\mathrm{kHz}\ . \tag{1}$$

The samples were investigated holographically at all frequencies found. A standard holographic arrangement was used with He-Ne laser ($\lambda = 633$ nm) and with pin-hole space filters, so that illuminating beam had the form of spherical wave. The photographic recording at holographic reconstruction was carried out with small aperture stop. The sample was fastened on its perimeter in an elastic holder rotatable around its vertical axis, so that holograms at its various angle positions could be recorded.

It is principially impossible to investigate the in-plane vibrations by using the sensitivity vector $\boldsymbol{s}$ [6]

(this vector halves the angle between illuminating and observation rays in the given point of the object) with the optimum orientation, parallel to the vibrational direction. In order to minimize angular deviation of **s** from the surface and, at the same time, to ensure a reasonable viewing angle of the plate in oblique projection, the arrangement according to fig. 1 was used. The position of the plate is characte-

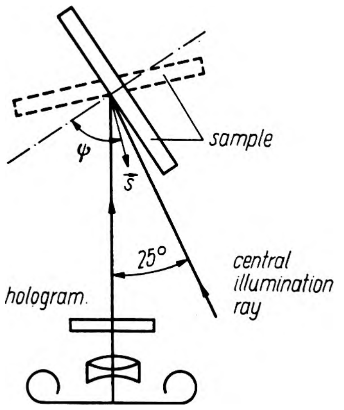

Fig. 1. Orientation of the sample in the experimental arrangement

rized by the angle ψ between its rotational axis and the vector **s**. To visualize the radial vibrations the angle ψ was adjusted up to 70°, whilst to observe the vibrations perpendicular to the surface the $\psi = 0°$ was taken as optimum (see the plate sketche din dashed line in fig. 1).

Holograms of the vibrating states of the thin plate were recorded at $\psi = 70°$. Their holographic recon-

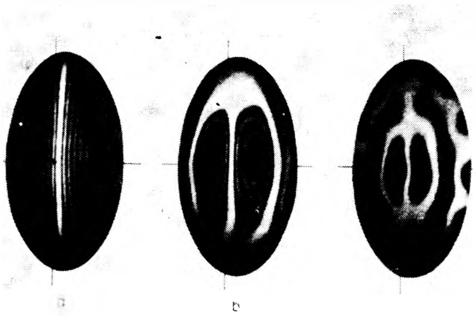

Fig. 2. Experimental interferograms of vibrations of thin plate ($t = 2$ mm) for orientation $\psi = 70°$:

a) $f_r = 47$ kHz, RMS value of exciting current $I = 400$ mA, b) $f_r = 125$ kHz, $I = 280$ mA, c) $f_r = 200$ kHz, $I = 220$ mA

structions, i.e. experimental interferograms (EI), are presented in fig. 2. Herein and in further EIs the centre of the face is denoted with a cross. For the thick plate only interferograms of the first vibration state are presented in figs 3 and 4 which correspond to two different magnitudes of the exciting amplitude and to $\psi = 65°$ and 0°.

At a first glance, the interference patterns for $\psi = 70°$ and 65° (figs 2, 3a, 4a) differ substantially from those of the radial vibrations. The circular

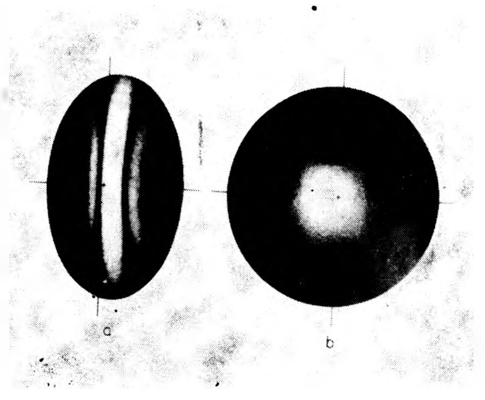

Fig. 3. Experimental interferograms of vibrations of thick plate ($t = 8$ mm) at the frequency $f_r = 46.5$ kHz and exciting current $I = 150$ mA

a) $\psi = 65°$, b) $\psi = 0°$

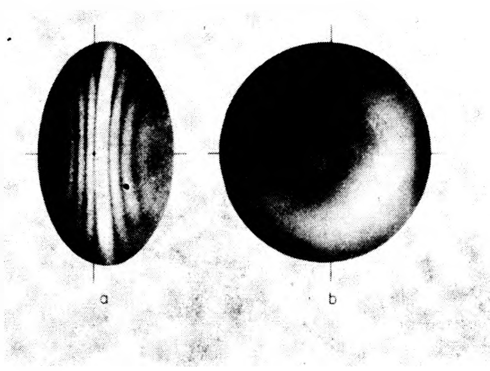

Fig. 4. The same as in fig. 3 with exception of exciting current $I = 300$ mA

symmetry of the amplitude is not reflected in the shape of the fringes, since the angle between the vector of the amplitude and the sensitivity vector varies substancially (roughly in the limits $90° \pm \psi$). All surface points in which this angle takes the value 90° constitute the zero order bright fringe having a slightly bent form because of the central illumination and observation. Obviously, this fringe represents a virtual knot-line and it must pass through the real knot-point with zero amplitude, i.e. through the centre of the plate surface.

However, an apparent shift of the zero-order bright fringe away from the centre can be seen on all EIs. This fact indicates the presence of another vibrations connected with the radial ones. As the circular symmetry must be preserved, these additional vibrations are perpendicular to the surface. On the other hand, the thickness vibration modes can occur only at much higher frequencies [5]. Because of the amplitude independence of zero-order-fringe shift (cf. figs 3 and 4) we hold these thickness vibrations for a manifestation of the transverse contraction being a consequence of the areal dilatation which corresponds to the radial vibrations.

Both the changing direction of sensitivity vector and the additional thickness vibrations make the evaluation of our EIs rather complicated. That is the reason for making use of the method of comparison of EIs with theoretical interferograms.

3. Model interferograms

What we call the model interferogram (MI) is the calculated fringe pattern covering the projection of the given object and corresponding exactly to the geometrical arrangement of the experiment as well as to the assumed vibrations of the object. For construction of the MI the graphic-numerical method EQUIDIF I [7] is used.

An approximate theory of contour vibrations of an isotropic thin circular plate has been dealt with by several authors [8–10]. The radial dependence of the amplitude of radial vibrations can be expressed in the form

$$a_r(r) = a\,\frac{J_1\left(x_k \frac{r}{R}\right)}{J_{1\max 1}}, \tag{2}$$

J_1 is the Bessel function of the first kind and first order, $J_{1\max 1} = J_1(1.84) = 0.582$ is the value in the first maximum of this function, and x_k is the k-th root of frequency equation

$$J_0(x_k) - (1-\sigma)\frac{J_1(x_k)}{x_k} = 0; \tag{3}$$

for $\sigma \approx 0.30$ first three radial modes correspond to: $x_1 \approx 2.05$, $x_2 \approx 5.39$, $x_3 \approx 8.57$ [5]. As it follows from eq. (2), a_r is the maximum amplitude of radial vibrations which for a particular mode occurs at the radius

$$r_{0k} \approx 1.84\frac{R}{x_k}. \tag{4}$$

The eq. (2) is depicted for $k = 1, 2, 3$ in fig. 5.

The amplitude of thickness vibrations can be expressed from the relation between thickness con-

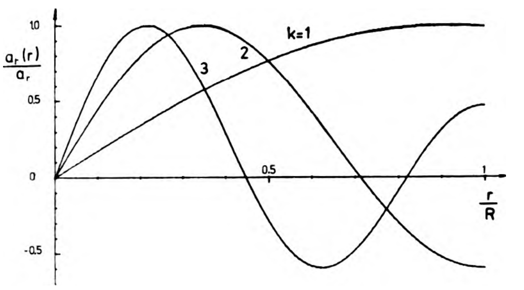

Fig. 5. Theoretical radial dependence of radial component of vibrations after eq. (2) for three lowest radial modes

traction δ_t and radial as well as tangential dilatations δ_r, and δ_φ, respectively:

$$\delta_t = -\sigma(\delta_r + \delta_\varphi) = -\sigma\Delta; \tag{5}$$

Δ denotes the areal dilatation. Provided that the transversal displacement in central plane of the plate equals zero, the amplitude of vibrations on the surface is

$$a_t(r) = \delta_t\frac{t}{2} = -\sigma\frac{t}{2}\,\Delta(r). \tag{6}$$

As follows from [8], in our case the relation

$$\Delta(r) = \frac{\partial a_r(r)}{\partial_r} + \frac{a_r(r)}{r_r} \tag{7}$$

takes place, which leads to the result

$$a_t(r) = a_r\sigma\frac{t}{2}\frac{x_k}{R}\,\frac{J_0\left(x_k\frac{r}{R}\right)}{J_{1\max 1}} = a_t J_0\left(x_k\frac{r}{R}\right). \tag{8}$$

This dependence is depicted for $k = 1, 2, 3$ in fig. 6. Let us note that the amplitude $a_t(r)$ has its maximum

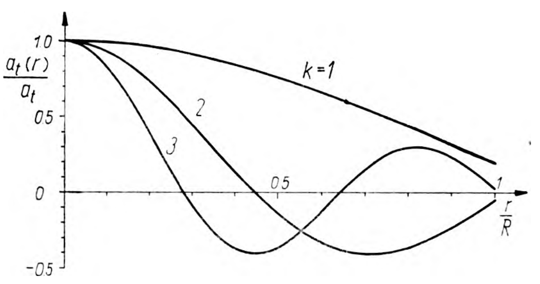

Fig. 6. Theoretical radial dependence of thickness component of vibrations after eq. (8) for three lowest radial modes

a_t in the centre of the plate; a_t is proportional to a_r:

$$a_t = pa_r. \tag{9}$$

MIs were constructed on the basis of eqs. (2) and (8), i.e. for the given k and depending on the parameters a_r and p. As long as MIs and EIs are in good qualitative agreement, the parameters a_r and p were also fitted in order to obtain a quantitative agreement. As the shift of the zero-order bright fringe in MIs depends on the value of p only, this value can be determined directly by reading the shift on EIs in figs. 2, 3, and 4. Then, having found the MI for a definite value of p and for an arbitrary value of a_r, we started with a dark fringe of higher order readable on the EI, and determined the change of a_r needed to transfer the corresponding fringe on MI into the same position.

In this way the MI was constructed which corresponds to fig. 2a ($k = 1$) for $a_r = 2.2$ and $p = 0.40$ (see fig. 7a). Herein the dimensionless amplitude a_r

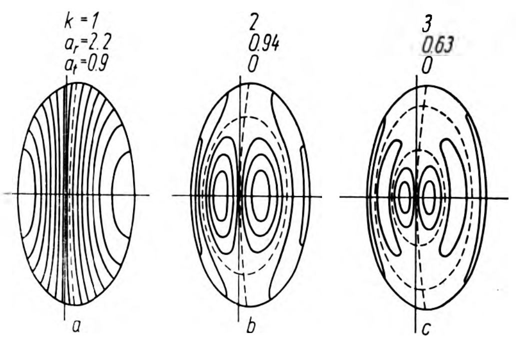

Fig. 7. Model interferograms corresponding to experimental ones in fig. 2 (thin plate, $\psi = 70°$)

is expressed in wavelengths of laser light used. For $k = 2$ and 3 in fig. 2b,c even qualitative agreement is not satisfactory, so that only approximate MIs were constructed for $p = 0$, and $a_r = 0.94$ and 0.63 (see figs 7b and c, respectively).

For thick sample (figs 3 and 4) identification of MIs with EI was performed for the orientation $\psi = 65°$ (see figs 8a and 9a) yielded $p = 0.41$, and $a_r = 0.73$ and 1.23, respectively. With these values of parameters, the MIs were also constructed for orientation $\psi = 0°$ (see figs 8b and 9b).

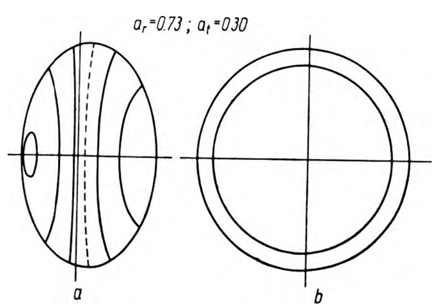

Fig. 8. Model interferograms corresponding to experimental ones in fig. 3

(thick plate, a) $\psi = 65°$, b) $\psi = 0°$)

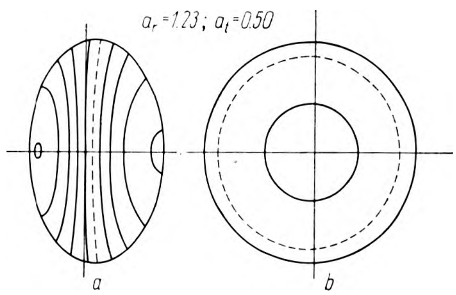

Fig. 9. Model interferograms corresponding to experimental ones in fig. 4

(thick plate, a) $\psi = 65°$, b) $\psi = 0°$)

4. Discussion

The comparison with MIs makes us sure that our EIs really represent radial vibration modes. In EIs of the thin plate (fig. 2) the interference pattern appears to be unsymmetrical against horizontal axis due to the violation of circular symmetry of the amplitude distribution, caused probably by the inhomogeneity of ceramic material or by imperfect clamping in the holder. Moreover, the EIs of higher radial modes ($k = 2,3$; see fig. 2b,c) are distorted by superimosed higher contour modes of C-type [10, 11]. Nevertheless, the characteristic features of the radial modes, i.e. one or two concentric knot-circles, are well distinguishable. Also the resonant frequencies of these vibration states are roughly proportional to the sequence of roots of the frequency equation (3).

More detailed analysis can be performed with the thick sample (figs 3, 4). MIs for $\psi = 65°$ (figs 8a, 9a), as well as the MIs for $\psi = 0°$ (figs 8b, 9b) which were constructed on the basis of the same values of parameters a_r and p, are in a good agreement with the corresponding EIs. In the latter case, slightly larger diameters of computed fringes reflect probably the low precision of readjustment of the vibration state at recording of the hologram from which the EI in fig. 4b was later reconstructed.

From our results it follows that — even with well pronounced radial vibrations — the nonradial (i.e. thickness) component is considerably large so that such vibrations cannot be taken for in-plane ones. The method of comparison the EIs with MIs made easier the evaluation of that complicated vibration state. Even in such relatively simple cases, it proved to be most advantageous to work with EIs by recording the given vibration state with several (at least two) different sensitivity vectors. It must be pointed out that a simultaneous recording of corresponding holograms is of a great importance. Otherwise, the poor reproduction of the vibration state under consideration can be hardly excluded and the results of analysis are doubtfull.

A drawback of the interferometric method used by us is the "a posteriori" recognition of the vibration state, i.e. the fact that the recognition of the vibration state earlier recorded in the interferogram is possible first at the reconstruction stage. To be sure at the very begining that the desirable vibration state is recorded some of the real-time interferometric methods should be used.

In these cases in the hologram only the still-stand state of the object is recorded, and the vibrating object is observed through the hologram being reconstructed simultaneously. Under such conditions, the surface of the object is covered with interference fringes. Their contrast, however, is very low and it decreases quickly with the order of the fringe [12]. Therefore the stroboscopic variant of the method appears to be more effective, giving the contrast of the fringes independently of the fringe order. The latter method uses short pulses of laser light both for reconstruction of the hologram and illumination of the vibrating object. The pulses are synchronized with the vibrations. Thus, in both the cases a proper vibrating state can be choosen visually in order to record the interferogram photographically.

5. Conclusions

The proposed experimental arrangement for holographic interferometric investigation of the vibrations with the amplitude vector having major component in the surface plane of the object, as well as the method of model evaluation of the interferograms proved to be satisfactory.

The so-called radial vibration modes of two circular piezoceramic plates were investigated. The distribution of the radial component of the amplitude showed a good agreement with the theory. The determined thickness component of the amplitude appears to be in accordance with elastic properties of the plates. The magnitudes of the both components were measured.

Радиальные колебания пьезокерамических резонаторов, исследуемые методом голографической интерферометрии

Три наиболее низких вида колебаний круговых пьезокерамических пластинок исследовались методом интерферометрической голографии с усреднением по времени. Обсуждены условия эксперимента и выбран оптимальный вариант прибора. Получено удовлетворительное соответствие результатов теории радиальных колебаний. Исследовались колебания толщины, какими сопровождались радиальные колебания.

References

[1] Powell R. L., Stetson K. A., *Interferometric Vibration Analysis by Wavefront Reconstruction*, J. Opt. Soc. Am. **55**, 1593–1598 (1965).

[2] Stetson K. A., *Holographic Vibration Analysis*, Holographic Nondestructive Testing (Ed. R. K. Erf), Academic Press, New York—London 1974, pp. 181–220.

[3] Hirose Y., Tsuzuki Y., Iijima K., *Measurement of Contour Vibrations of Quartz Plates by Holographic Technique*, Electronics and Communications in Japan **53-A**, No. 6 49–55, (1970).

[4] Chomát M., Miler M., *Application of Holography to the Analysis of Mechanical Vibration of Electronic Components*, TESLA Electronics **6**, 83–93 (1973).

[5] Hiršl J., Černohlávek D., Stefan O., Čermák F., *Ceramic Piezoelectrics*, TESLA — VÚST, Praha 1970 (In Czech).

[6] Stetson K. A., *Fringe Interpretation for Hologram Interferometry of Rigid-Body Motions and Homogeneous Deformations*, J. Opt. Soc. Am. **64**, 1–10 (1974).

[7] Janta J., Miler M., *Model Interferogram as an Aid for Holographic Interferometry*, J. of Optics (Paris) **8**, XXX–XXX (1977).

[8] Love A. E. H., *A Treatise on the Mathematical Theory of Elasticity*, Cambridge 1927, pp. 497–498.

[9] Petržílka V., *Längsschwingungen von kreisförmigen Quarzplatten*, Ann. der Physik **5**, Folge 23, 156–168 (1935).

[10] Onoe M., *Contour Vibrations of Isotropic Circular Plates*, J. Acoust. Soc. Am. **28**, 1158–1162 (1956).

[11] Stefan O., *Contour Oscillations of Circular Ceramic Resonators*, Československý Časopis pro Fyziku **A 20**, 113–122, (1970) (In Czech).

[12] Listovets V. S., Ostrovskii Yu. I., *Interference-holographic Methods of Vibration Analysis*, Zh. Tech. Fiz. **44**, 1345–1406, (1974) (In Russian).

Received, May 5, 1977